Plant Physiology®

https://doi.org/10.1093/plphys/kiae419 Advance access publication 14 August 2024

Research Article

Outward askew endodermal cell divisions reveal INFLORESCENCE AND ROOT APICES RECEPTOR KINASE functions in division orientation

R.M. Imtiaz Karim Rony, ^{1,2} Roya Campos, ¹ Patricio Pérez-Henríquez, ^{1,3} D Jaimie M. Van Norman ^{1,2,3,*} D

The author responsible for distribution of materials integral to the findings presented in this article in accordance with the policy described in the Instructions for Authors (https://academic.oup.com/plphys/pages/General-Instructions) is Jaimie M. Van Norman.

Abstract

Oriented cell divisions establish plant tissue and organ patterning and produce different cell types; this is particularly true of the highly organized Arabidopsis (Arabidopsis thaliana) root meristem. Mutant alleles of INFLORESCENCE AND ROOT APICES RECEPTOR KINASE (IRK) exhibit excess cell divisions in the root endodermis. IRK is a transmembrane receptor kinase that localizes to the outer polar domain of these cells, suggesting that directional signal perception is necessary to repress endodermal cell division. Here, a detailed examination revealed many of the excess endodermal divisions in irk have division planes that specifically skew toward the outer lateral side. Therefore, we termed them "outward askew" divisions. Expression of an IRK truncation lacking the kinase domain retains polar localization and prevents outward askew divisions in irk; however, the roots exhibit excess periclinal endodermal divisions. Using cell identity markers, we show that the daughters of outward askew divisions transition from endodermal to cortical identity similar to those of periclinal divisions. These results extend the requirement for IRK beyond repression of cell division activity to include cell division plane positioning. Based on its polarity, we propose that IRK at the outer lateral endodermal cell face participates in division plane positioning to ensure normal root ground tissue patterning.

Introduction

In multicellular eukaryotes, cell division produces diverse cell types and increases cell number for body plan elaboration and growth. Cell divisions are typically categorized as proliferative (symmetric) and formative (asymmetric). Proliferative cell divisions are typically physically symmetrical, producing daughter cells of the same size and cell identity. In contrast, formative cell divisions can be physically symmetrical or asymmetrical but the daughter cells acquire distinct identities. Due to the cell wall, the relative position of individual plant cells is fixed in space, as such, previous division orientations are "recorded" by the placement of the walls (Facette et al. 2018; Rasmussen and Bellinger 2018). The orientation of plant cell divisions is informed by extracellular cues and intracellular polarized proteins and is crucial for plant cell fate determination and tissue organization (Rasmussen et al. 2011; Van Norman 2016; Wallner 2020; Hartman and Muroyama 2023). Because the developmental trajectory of a daughter cell is influenced by positional information (van den Berg et al. 1995; Marhava et al. 2019), division plane orientation is a key developmental decision.

The orientation of plant cell divisions is defined by how the new cell wall is positioned relative to the surface of the organ (Livanos and Müller 2019). Accordingly, periclinal cell divisions are oriented parallel to the surface and anticlinal cell divisions are oriented perpendicular to the surface. For anticlinal cell divisions, the division plane can be aligned with the organ's longitudinal

or transverse axis (Fig. 1, A and B); therefore, we distinguish between longitudinal anticlinal and transverse anticlinal cell divisions. In the root, periclinal cell divisions are typically formative as they generate additional layers of distinct cell types (De Smet and Beeckman 2011; Pillitteri et al. 2016). However, anticlinal cell divisions are often proliferative, generating more cells of the same type. Normal tissue and organ patterning require the specific orientation of proliferative and formative cell divisions relative to the plant body axes. Yet our understanding of how division plane orientation is precisely controlled and how it is coupled with cell division frequency remains limited.

The highly stereotypical cellular organization of the Arabidopsis (Arabidopsis thaliana) root makes it an ideal system to investigate how the frequency and orientation of cell division contribute to tissue/organ patterning. The root ground tissue (GT) is a good example of how a specific series of oriented formative cell divisions give rise to distinct cell types, the cortex and endodermis. First, the GT stem cell, the cortex/endodermal initial [CEI (Fig. 1, A and B)], undergoes a formative, transverse anticlinal division to produce the CEI daughter cell (CEID). This daughter cell then undergoes a formative, periclinal division to produce endodermis toward the inside and cortex toward the periphery of the root [Fig. 1B (Dolan et al. 1993; Scheres and Benfey 1999)]. As plants mature, endodermal cells can undergo another periclinal division to produce another cortex layer called the middle or secondary cortex (Paquette and Benfey 2005; Cui 2016). After their

¹Department of Botany and Plant Sciences, Institute of Integrative Genome Biology, University of California, Riverside, California 92521, USA

²Department of Molecular, Cell, and Systems Biology, Center for Plant Cell Biology, Institute of Integrative Genome Biology, University of California, Riverside, California 92521, USA

³Department of Molecular, Cell & Developmental Biology, University of California, Los Angeles, California 90095 , USA

^{*}Author for correspondence: jaimievannorman@ucla.edu (J.M.V)

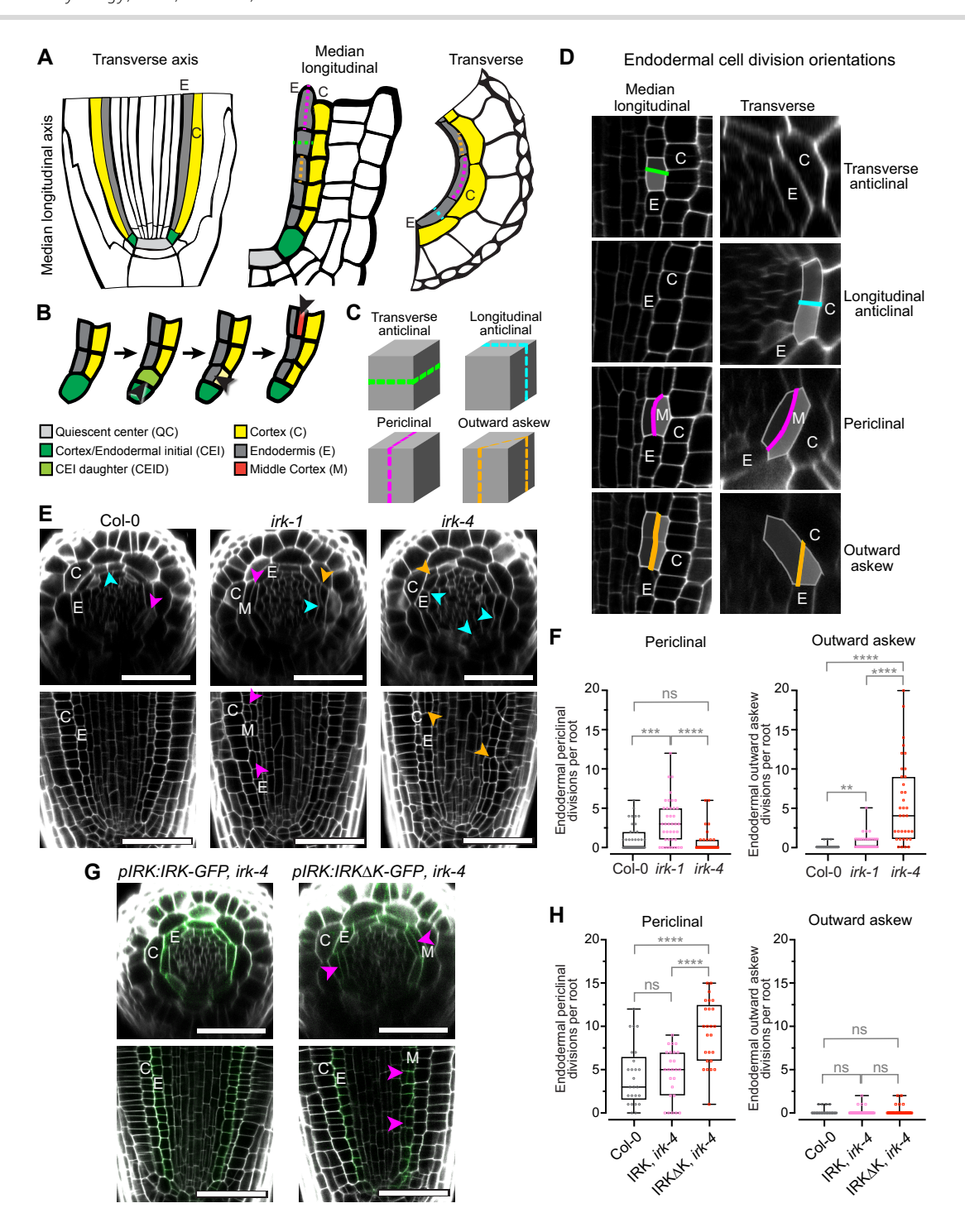


Figure 1. Arabidopsis root cellular organization, cell division plane orientations, and irk phenotypes. A) Schematic of a root tip (left) with ground tissue cell files and quiescent center (QC) highlighted and root axes indicated. Closeup views of (center) a median longitudinal and (right) transverse sections with endodermal division orientations indicated by dotted lines. B) Schematic of ground tissue cell divisions to form endodermis (E), cortex (C), and middle cortex (M). Arrowheads indicate formative cell divisions. C) Schematics of division orientations with single endodermal cells represented as cubes. D) Confocal micrographs showing different orthogonal views [median longitudinal (left) and transverse (right)] of endodermal cells that have undergone a cell division in each orientation. Note transverse anticlinal divisions are not visible in the longitudinal axis. E) Confocal micrographs showing transverse sections (upper) and median longitudinal sections (lower) of root tips stained with propidium iodide (PI, gray) with excess endodermal cell divisions indicated by colored arrowheads: periclinal (magenta), longitudinal anticlinal (cyan), and outward askew (orange). F) Quantification of the total number of periclinal and outward askew divisions per genotype (n = 35 to 40 roots per genotype). Graphs show the combined results from 3 replicates. G) Confocal micrographs showing transverse sections (upper) and median longitudinal sections (lower) of irk-4 expressing (left) pIRK:IRK-GFP and (right) pIRK:IRK/MK-GFP stained with PI (gray) merged with green fluorescent protein (GFP, green). H) Quantification of total number of periclinal and outward askew divisions in each genotype (n = 25 roots per genotype). Graphs show results combined from two replicates. Box plots in F, H showing total number of divisions per root with whiskers indicating min/max with interquartile range and median shown with black boxes/lines, respectively; Col-0: gray circles, irk-1: pink squares, and irk-4: red squares. Statistics in

formation, cortex and endodermal cells proliferate through symmetrical, transverse anticlinal divisions, producing more cells in their respective longitudinal files. Symmetrical, longitudinal anticlinal divisions (LADs) can also occur producing more GT cells in the root's radial axis (Fig. 1A), however, these divisions are rarely observed in young wild-type roots, and as a result, 8 of each GT cell type, including the CEI, are most often observed around the stele (Dolan et al. 1993; Scheres and Benfey 1999). Deviations in cell division planes lead to irregular daughter cell shapes allowing the consequences of misoriented root cell divisions to be followed in time and space.

Strict regulation of GT cell division in the root's radial axis is disrupted in mutant alleles of IRK (INFLORESCENCE AND ROOT APICES RECEPTOR KINASE), which exhibit excess endodermal longitudinal anticlinal and periclinal cell divisions (Campos et al. 2020). These excess cell divisions coincide with promoter activity of CYCLIN D6; 1 (Campos et al. 2020), a specific D-type cyclin, associated with formative, but not proliferative, GT cell divisions (Sozzani et al. 2010). Yet, no increase in proliferative, transverse anticlinal divisions was observed in irk-4, suggesting IRK specifically represses cell divisions that produce more cells in the root's radial axis (Campos et al. 2020). We propose that IRK specifically represses an endodermal cell division program that widens the GT and that longitudinal anticlinal and periclinal endodermal cell divisions are developmentally regulated downstream of IRK.

IRK encodes a transmembrane receptor kinase of the Arabidopsis RECEPTOR-LIKE KINASE (RLK) superfamily (Shiu and Bleecker 2001; Shiu and Bleecker 2003), which accumulates to the outer polar domain of the endodermal plasma membrane (PM). Although IRK is expressed in several root cell types, endodermal-specific expression of IRK is sufficient to rescue the cell division defects in irk (Campos et al. 2020; Rodriguez-Furlan et al. 2022). Unexpectedly, IRK maintains its polar localization when the intracellular domains are missing and the IRK truncation remains largely functional, rescuing the endodermal LADs but not the periclinal divisions in irk-4 (Rodriguez-Furlan et al. 2022). Polar accumulation of IRK to the outer lateral endodermal cell face suggests it perceives extracellular information that originates peripheral to the endodermis and is required to maintain GT organization and cell number in the root's radial axis. However, the molecular details of IRK function remain unclear.

Here, we closely examined the excess endodermal divisions in irk mutants and identified a distinct cell division orientation defect. Unexpectedly in irk-4, a null allele, the majority of endodermal cell divisions previously characterized as periclinally oriented, instead, have outwardly skewed division planes. We defined these as "outward askew" endodermal divisions, because these oblique divisions consistently produce small, abnormally shaped cells peripheral to the endodermis. In the weaker irk-1 allele, roots have fewer outward askew endodermal cell divisions, but have excess longitudinal anticlinal and periclinal divisions. Therefore, while both irk alleles have excess GT cells in the radial axis, the orientation of the excess cell divisions is different. Additionally, the IRK intracellular truncation prevents the excess outward askew endodermal divisions in irk-4, but excess periclinal divisions are present, phenocopying irk-1. These results expand the function of IRK beyond repression of endodermal cell division activity showing it is also required for cell division plane orientation. Given its polar accumulation in the PM, IRK may participate in division plane orientation through physical involvement with cell division machinery or through perception of directional, positional information. We propose a

model whereby the presence of IRK at the outer polar domain occludes that endodermal cell face for division plane selection or cell plate attachment.

Results

Many endodermal cell divisions in irk-4 are abnormally oriented

Close examination of endodermal cell division orientation in irk-4 revealed that the divisions we had classified as periclinal were not oriented parallel to the root's surface. If a periclinal division is considered in 2 dimensions (2D) in the longitudinal axis, the new cell plate attaches to opposite root/shootward endodermal faces within a cell file. However, in irk-4, we observed abnormal divisions where cell plates attach to adjacent endodermal faces the shoot- or rootward face and the outer lateral face (Fig. 1, C to E). These abnormal, oblique division planes resulted in new cell walls that often appeared periclinally oriented when viewed only in longitudinal optical sections. However, in 3D, as observed in a series of longitudinal and transverse optical sections [in confocal z-stacks (Campos and Van Norman 2022)], key differences between true periclinal and these abnormal divisions become apparent. Periclinal endodermal divisions produce daughter cells of nearly equal size, whereas the abnormal divisions in irk-4 result in unequal daughter cell sizes with the smaller, prism-shaped cell peripherally positioned. Intriguingly, we did not observe any abnormal divisions oriented toward the inner lateral side of the endodermis, indicating division planes in irk-4 are not randomly misoriented. Given the specific orientation of these divisions, we termed them outward askew endodermal divisions.

To assess the frequency of outward askew endodermal divisions, we examined a set of confocal images (Rodriguez-Furlan et al. 2022) to specifically parse outward askew from periclinal endodermal divisions. This revealed that 88.8% of the endodermal divisions in irk-4 classified as periclinal (n = 224 divisions) were outward askew divisions. Thus, there was no significant difference in the number of periclinal divisions in irk-4 compared to wild type [Wt (Fig. 1F)]. In young Wt roots, periclinal divisions are somewhat rare and 5.1% of the divisions classified as periclinal (n = 59 divisions) were found to be outward askew. In irk-1, a partial loss of function allele, we found that 15.6% of divisions classified as periclinal (n = 154 divisions) are outward askew oriented. Despite this, irk-1 roots have significantly more periclinal divisions than Wt (Fig. 1F). These analyses revealed key phenotypic differences between the irk alleles: irk-4 has substantially more outward askew and longitudinal anticlinal divisions than Wt or irk-1, whereas irk-1 has significantly more periclinal and longitudinal anticlinal divisions than Wt. Because irk-1 has significantly fewer outward askew endodermal divisions than irk-4 (Fig. 1F), these divisions appear to be a specific phenotype observed upon complete loss of IRK function. These observations indicate that IRK operates not only to repress endodermal cell division activity but also functions in division orientation.

The IRK kinase domain is dispensable for its role in cell division orientation

We previously showed that truncations of IRK missing the intracellular domains maintained their polar accumulation in all root cell types examined (Rodriguez-Furlan et al. 2022). Specifically, IRK missing its kinase domain (IRKAK-GFP) was polarly localized in the root endodermis (Fig. 1G) and, while it fully rescued the irk-4 endodermal LAD phenotype; it did not rescue

the periclinal division phenotype (Rodriguez-Furlan et al. 2022). This is reminiscent of the irk-1 root phenotype. As the irk-1 allele contains a T-DNA insertion near the beginning of the region coding for the kinase domain (Campos et al. 2020), we predict that the production of a partially functional truncation results in the milder irk-1 cell division phenotype. The IRKAK truncation was designed to match the remaining endogenous sequence in the irk-1 allele. With the recent detection of additional phenotypic consequences of irk loss of function and differences between the irk alleles, we investigated whether IRKAK-GFP could rescue the outward askew cell division phenotype of irk-4.

We found that irk-4 roots expressing the full-length IRK-GFP or IRKAK-GFP showed rescue of endodermal LAD and outward askew phenotypes (Fig. 1, G and H). However, the irk-4 IRKΔK-GFP roots had significantly more periclinal endodermal divisions than Wt or irk-4 IRK-GFP plants, making them phenotypically similar to irk-1. This indicates presence of IRKAK at the outer polar domain is sufficient to repress longitudinal anticlinal and outward askew endodermal divisions in irk-4, but cannot prevent excess periclinal divisions. Thus, although excess endodermal divisions are present in irk-4 IRKAK-GFP roots, they are predominantly periclinally oriented, which is more typical for endodermal formative divisions (Paquette and Benfey 2005; Cui 2016). These observations suggest the IRK kinase domain is largely dispensable in endodermal division plane orientation, but is involved in repression of endodermal cell division activity.

Outward askew endodermal cell divisions in irk-4 coincide with CYCD6; 1 promoter activity

In Wt roots, formative GT cell divisions are associated with promoter activity of a specific D-type cyclin, pCYCD6; 1, this includes divisions of the initial cells and periclinal endodermal divisions, which generate middle cortex (Sozzani et al. 2010). In irk mutants, excess endodermal LADs also coincide with pCYCD6; 1 activity (Campos et al. 2020). This putatively links longitudinal anticlinal and periclinal endodermal divisions through some shared regulatory mechanism(s) downstream of IRK function and suggests IRK specifically represses an endodermal cell division program that operates in the root's radial axis.

With the addition of outward askew divisions to the population of excess endodermal divisions in irk-4, we conducted a detailed examination of pCYCD6; 1:erGFP expression in irk and Wt roots grown on 0.2 x MS, which aggravates irk root phenotypes (Campos and Van Norman 2022; Goff et al. 2023). Similar to our previous report, pCYCD6; 1 activity is substantially increased in the irk endodermis compared to Wt. We quantified abnormal endodermal cell divisions together with the expression of pCYCD6; 1:erGFP and mapped this information in the root's longitudinal axis (Figs. 2, 3 and Supplementary Fig. S1). In Wt roots, endodermal LADs occur much less frequently than in irk and the daughter cells are rarely associated with pCYCD6; 1 activity (Fig. 2, A to D). Under these conditions, periclinal divisions occur in Wt at this age (6 days post-stratification) and, as expected, often associate with pCYCD6; 1 activity (Supplementary Fig. S1, A to D). In irk-1, there are more endodermal LADs than in Wt with daughter cells frequently showing pCYCD6; 1 activity. irk-4 roots have endodermal LADs at nearly every position in the longitudinal axis, and with rare exception, these daughter cells show pCYCD6; 1 activity (Fig. 2, C and D). Like in Wt, periclinal endodermal divisions in irk alleles most often associated with pCYCD6; 1 activity (Supplementary Fig. S1, C and D). These results reveal extensive excess endodermal LADs in irk mutants and confirm their strong association with pCYCD6; 1 activity.

Outward askew endodermal cell divisions are also associated with pCYCD6; 1 activity (Fig. 3). In the rare instances when outward askew divisions are observed in the Wt endodermis, they are associated with pCYCD6; 1 activity (Fig. 3, A to C). This association was also observed in irk mutants, where there are numerous outward askew endodermal divisions (Fig. 3, B and C). In Wt and irk-1, outward askew endodermal divisions begin to occur 5 or more cells above the quiescent center (QC); however, in irk-4, outward askew divisions occur much more frequently and closer to the QC (Fig. 3C). Like endodermal LADs in irk, the daughter cells of outward askew divisions nearly always show pCYCD6; 1 activity (Fig. 3, B and C). Altogether, our endodermal cell division maps reveal extensive excess endodermal cell divisions in the irk mutants, particularly in irk-4, where the daughter cells of LADs and outward askew divisions consistently show pCYCD6; 1 activity. The association of pCYCD6; 1 activity with each of the excess endodermal cell division orientations in irk further demonstrates the requirement for IRK in repression of cell division activity in the endodermis.

Peripheral daughter cells of outward askew endodermal divisions often express a marker of cortex identity

Endodermal periclinal, longitudinal anticlinal, and outward askew cell divisions all result in an increased number of GT cells in the radial axis of irk roots. LADs produce more endodermal cells around the stele and periclinal divisions produce a third GT layer, the middle cortex. We expect that the daughters of endodermal LADs will maintain endodermal identity, while those of periclinal divisions will transition to cortex identity (Figs. 4, Supplementary Figs. S2, and S3). As endodermal outward askew cell divisions produce peripherally located, prism-shaped cells of unknown fate, we examined reporter gene expression for endodermal and cortex cell identity (Fig. 4). We first examined SCARECROW promoter activity (pSCR:erGFP), which is expressed in endodermal cells throughout the root (Di Laurenzio et al. 1996; Wysocka-Diller et al. 2000). In Wt, 43% (3 of 7) of peripheral daughters of outward askew divisions show pSCR activity. In irk-1 and irk-4, 94% (25 of 26) and 60% (176 of 293) of these daughter cells show pSCR activity (Fig. 4, A to C), respectively. Thus, regardless of genotype, not all peripheral daughters of outward askew endodermal divisions show pSCR activity, implying they do not maintain endodermal identity.

Next, we examined the activity of the CORTEX2 promoter driving nuclear localized-yellow fluorescent protein (pCO2:nlsYFP), which is expressed in cortex cells in the root meristem (Heidstra et al. 2004; Paquette and Benfey 2005). In Wt roots, cells immediately peripheral to the endodermis have cortex identity (Fig. 1B), whether those cells are derived from periclinal CEID or endodermal divisions. Outward askew divisions were very infrequent in Wt and irk-1 expressing pCO2:nlsYFP. The single peripheral outward askew daughter in Wt did not express pCO2 and only one of 4 did in irk-1. In irk-4, ~21% (46 of 216) of the peripheral daughters of outward askew divisions exhibited pCO2 activity (Fig. 4, D to F). Comparison of the activity of pSCR and pCO2, particularly in irk-4, suggests that peripheral daughters of endodermal outward askew divisions gradually acquire cortex cell fate similar to what is observed for the peripheral daughters of endodermal periclinal divisions.

To more directly investigate this, we examined irk-4 roots simultaneously expressing pSCR and pCO2 reporters. Using linear unmixing, the daughters of endodermal longitudinal anticlinal, periclinal, and outward askew divisions were examined (Fig. 5, A to D). The daughter cells of endodermal LADs exclusively showed pSCR expression as expected, whereas the daughter cells

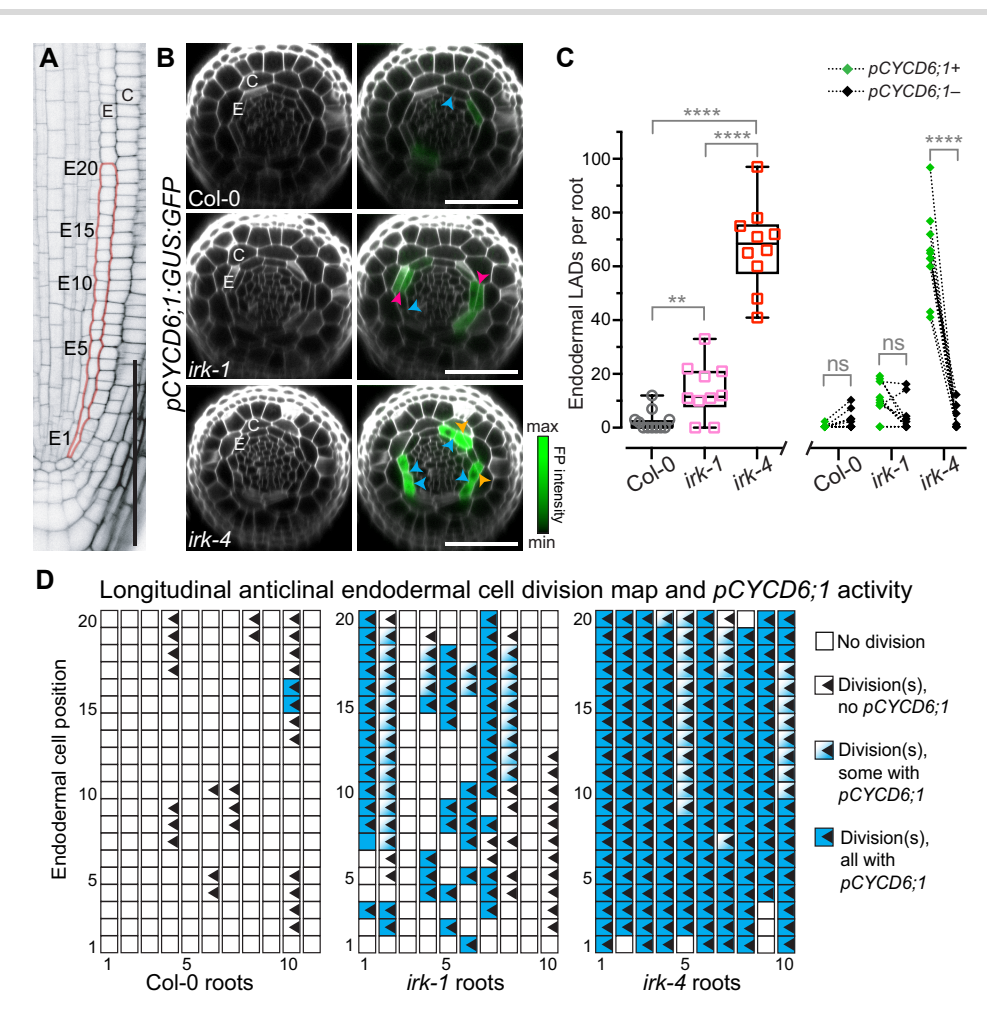


Figure 2. Longitudinal anticlinal endodermal cell divisions in irk often exhibit pCYCD6; 1 activity. A) Confocal micrograph of a median longitudinal section of a portion of the root meristem stained with propidium iodide (PI, gray) with an outline showing the first 20 endodermal (E) cells (E1 to 20) above the QC. B) Confocal micrographs of transverse optical sections of Arabidopsis root meristems at E10. Roots were stained with PI (gray, left panels) to visualize cells and merged with pCYCD6; 1:GUS:GFP activity (green fluorescent protein, right panels with intensity color scale at right). Endodermal cell divisions indicated by colored arrowheads: periclinal (magenta), longitudinal anticlinal (cyan), and outward askew (orange). Cortex (C) cell layer labeled for reference in A, B. Scale bars: $50 \,\mu\text{m}$. C) Box plot (left) showing the total number of endodermal longitudinal anticlinal divisions (LADs) per root with whiskers indicating min/max with interquartile range and median shown with black boxes/lines, respectively, and colored symbols show measurements for individual roots with Col-0: gray circles, irk-1: pink squares, and irk-4: red squares. Paired point graph (right) showing LADs in individual roots with (+, green diamonds) or without (-, black diamonds) pCYCD6; 1 activity. D) Cell division map for endodermal LADs in the first 20 endodermal cells above the QC. Data shown are from one representative replicate of \geq 2, 10 to 11 roots per genotype, with similar results. Statistics in C: ns = not statistically significant, P-values: ** < 0.01, **** < 0.0001, assayed by Mann–Whitney tests.

of periclinal and outward askew divisions showed expression of either or both of these markers (Fig. 5B). This suggests the daughter cells of outward askew and periclinal divisions progress along a similar developmental trajectory and supports the idea that outward askew divisions are formative divisions. Moreover, our observations suggest that pCO2 activity is progressively turned on in more distal peripheral daughters in files of these prism-shaped cells (Fig. 5C). Lastly, peripheral outward askew daughter cells more frequently show simultaneous pSCR and pCO2 activity, suggesting acquisition of cortex cell identity progresses more slowly than in the peripheral daughters of periclinal divisions (Fig. 5D). Overall, we find that peripheral outward askew daughters appear to gradually acquire cortex identity.

Outward askew and periclinal endodermal divisions often co-occur in the root's longitudinal axis

Root cell divisions typically bisect cells strictly parallel or perpendicular to the root surface. In 2D in the transverse axis, periclinal

endodermal divisions occur when a new cell plate meets the circumferential endodermal faces and LADs occur when the new cell plate meets the outer and inner endodermal faces. The resulting pair of daughter cells for each division are similarly sized, but periclinal divisions are formative and produce a new cell layer with a distinct fate (middle cortex, Fig. 1, A to C). In contrast, the daughters of endodermal LADs remain endodermal. Outward askew endodermal divisions are unique, with a division plane oblique to the root surface that creates daughter cells of different sizes, with the smaller prism-shaped cell consistently positioned peripherally. When considered in 2D in the transverse axis, these divisions occur when a new cell plate meets the outer lateral endodermal face and an adjacent circumferential endodermal face. Given the positions of cell plate attachment (Fig. 1C), outward askew divisions could simply be misoriented longitudinal anticlinal or periclinal endodermal cell divisions. To begin to address this, we assessed whether there was a spatial relationship between the excess endodermal cell division orientations in irk.

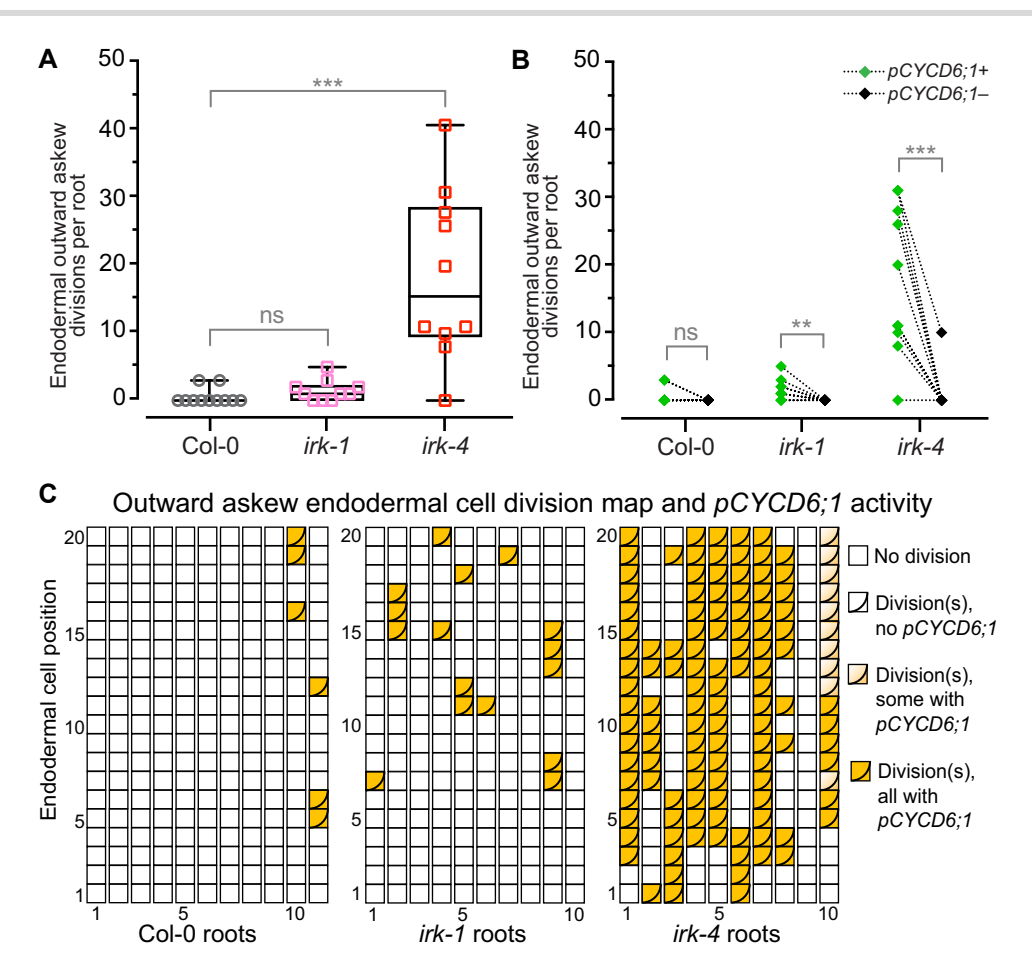


Figure 3. Outward askew endodermal divisions consistently show $pCYCLIN\ D6$; 1 activity. **A, B)** Quantification of outward askew endodermal divisions per root (the same roots examined as in Fig. 2). **A)** Box plot showing total number of outward askew divisions per root with whiskers indicating min/max with interquartile range and median shown with black boxes/lines, respectively, and colored symbols show measurements for individual roots with Col-0: gray circles, irk-1: pink squares, and irk-4: red squares. **B)** Paired point graph showing the number of outward askew divisions in individual roots with (+, green diamonds) or without (−, black diamonds) $pCYCLIN\ D6$; 1 (pCYCD6; 1) activity. **C)** Cell division map for endodermal outward askew divisions in the first 20 endodermal cell above the QC (n = 10 to 11 roots per genotype). Data shown from one representative replicate of ≥ 2, with similar results. Statistics in A, B: ns = not statistically significant, P-values: **<0.01, ***=0.001, assayed by Mann-Whitney tests.

Within individual cell files, we located endodermal outward askew divisions and assessed instances in which the adjacent shootward and/or rootward cell(s) had undergone a periclinal or longitudinal anticlinal division or had not divided at all (immediately adjacent outward askew divisions were not counted, Fig. 5E). In irk-1, outward askew endodermal divisions were adjacent to a periclinal division >60% of the time. Otherwise, the neighbor had not divided at all. In irk-4, outward askew divisions were most often adjacent to undivided endodermal cells and to periclinal divisions just over 30% of the time. Unexpectedly, outward askew divisions in irk-4 were rarely flanked by LADs (Fig. 5F). This is striking, because endodermal LADs in irk-4 are extremely numerous, whereas periclinal divisions and undivided cells are much less numerous (e.g. compare Fig. 2 and Supplementary Fig. S1 to Fig. 3). In Wt, outward askew endodermal divisions are very rare, just 2 instances were observed, with one case each in which the adjacent neighbor had divided periclinally and not at all. These results suggest that endodermal outward askew divisions are most often adjacent to cells that have divided periclinally or not divided at all. Given that endodermal outward askew daughter cells are peripherally located, transition to cortex identity, and their neighbors are more likely to have undergone a periclinal division, we propose outward askew divisions are not misoriented LADs, but are abnormal GT formative divisions.

Discussion

We have identified excess and obliquely skewed endodermal cell divisions in irk mutants, an aspect of the mutant phenotype that reveals IRK functions to repress endodermal cell division activity and is required for cell division orientation. Typically, endodermal cell divisions bisect the cell into similarly sized daughters, however, the divisions we define as outward askew have oblique division planes creating small prism-shaped cells. Of particular surprise is the invariable positioning of these smaller daughter cells toward the outer lateral side—nearer the cortex. If there were random misorientation of endodermal divisions in irk, we would expect that approximately half would be oriented toward the inner lateral side, such that the smaller daughter cells formed nearer the pericycle. Because this was not observed in any of our experiments, there is no support for random misorientation of endodermal cell division in irk; instead, these abnormal divisions have a specific orientation. This is consistent with a hypothesis where positional information orients cell division planes away from the lateral endodermal cell faces in Wt, but in irk mutants, information is missing and division planes frequently contact the outer lateral face.

The specific orientations of the excess divisions among irk alleles suggest endodermal division activity and orientation are

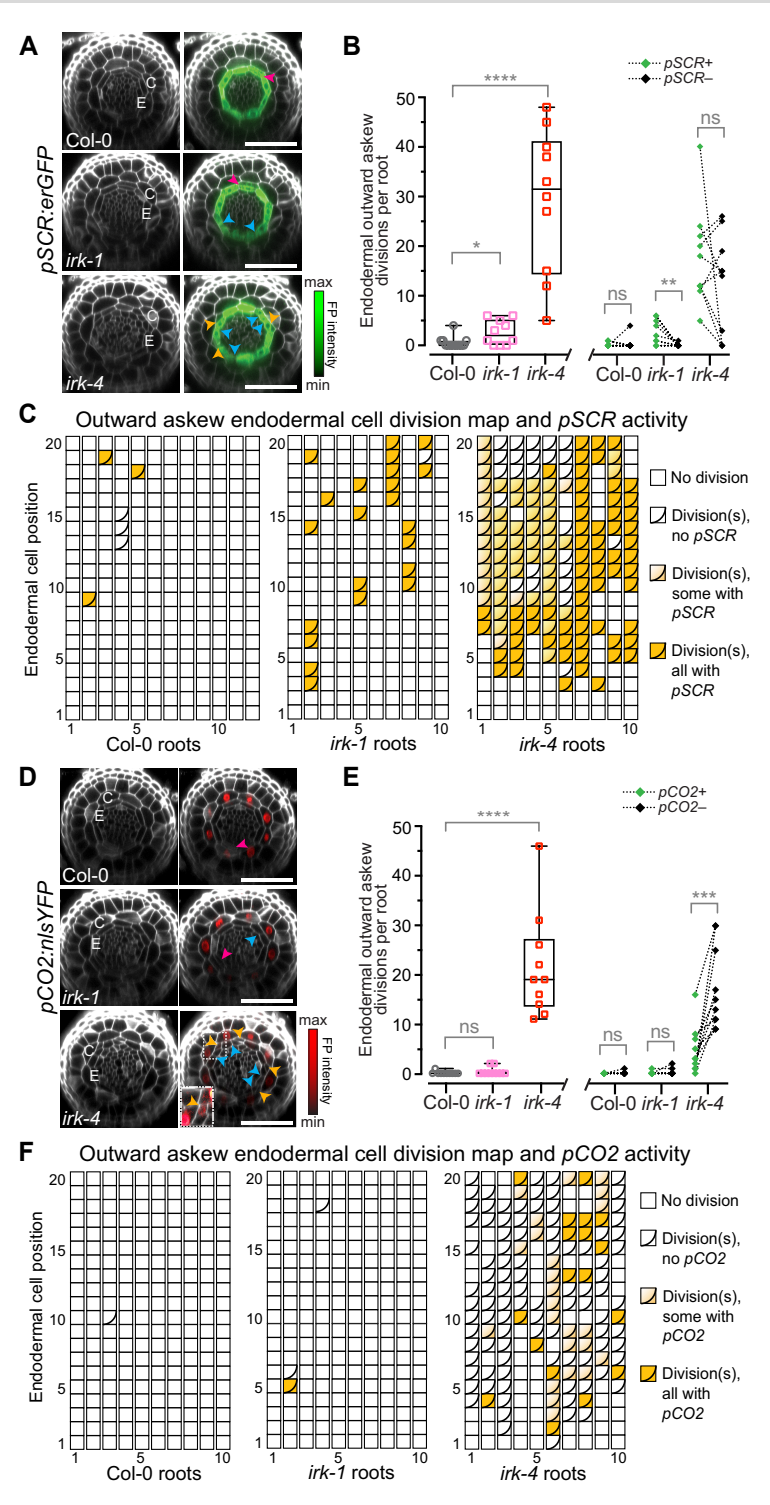


Figure 4. Outward askew division daughters and expression of ground tissue cell identity reporters. A, D) Confocal micrographs of transverse optical sections of Arabidopsis root meristems at position E10 with scale bars at 50 µm and endodermal (E) division orientations indicated by colored arrowheads: periclinal (magenta), longitudinal anticlinal (cyan), and outward askew (orange). Cortex (C) cell layer shown for reference in A, D) A) Images of roots expressing pSCARECROW: endoplasmic reticulum-green fluorescent protein (pSCR: erGFP) stained with propidium iodide (PI, gray, left) and merged with images of pSCR activity (color intensity scale, green to black, at right). B) Quantification of outward askew divisions per root and the numbers of outward askew divisions in individual roots with (+) or without (-) pSCR activity. C) Cell division map for endodermal outward askew divisions in the first 20 endodermal cells above the QC (n = 10 to 12 roots per genotype). D) Images of roots expressing pCORTEX2:nuclear localized yellow fluorescent protein (pCO2:nlsYFP) were stained with PI (gray, left) and merged with images of pCO2 activity (color intensity scale, red to black, at right). Inset shows outward askew daughter cell with signal adjusted to highlight pCO2 activity. Arrowheads as indicated for (A). E) Quantification of outward askew divisions per root and the numbers of outward askew divisions in individual roots with (+) or without (-) pCO2 activity. F) Cell division map for endodermal outward askew divisions (n = 10 roots per genotype). B, E) Box plots show total number of outward askew endodermal divisions per root with whiskers indicating min/max with interquartile range and median shown with black boxes/lines, respectively, and colored symbols show measurements for individual roots with Col-0: gray circles, irk-1: pink squares, and irk-4: red squares. Paired point graphs showing the number of outward askew divisions with (+, green diamonds) pSCR/pCO2 activity or without (-, black diamonds) pSCR/pCO2 activity. Data shown are from one representative replicate of ≥2, with similar results. Statistics in B, E: ns = not statistically significant, P-values: ** < 0.01, *** < 0.001, *** < 0.0001, assayed by Mann-Whitney tests.

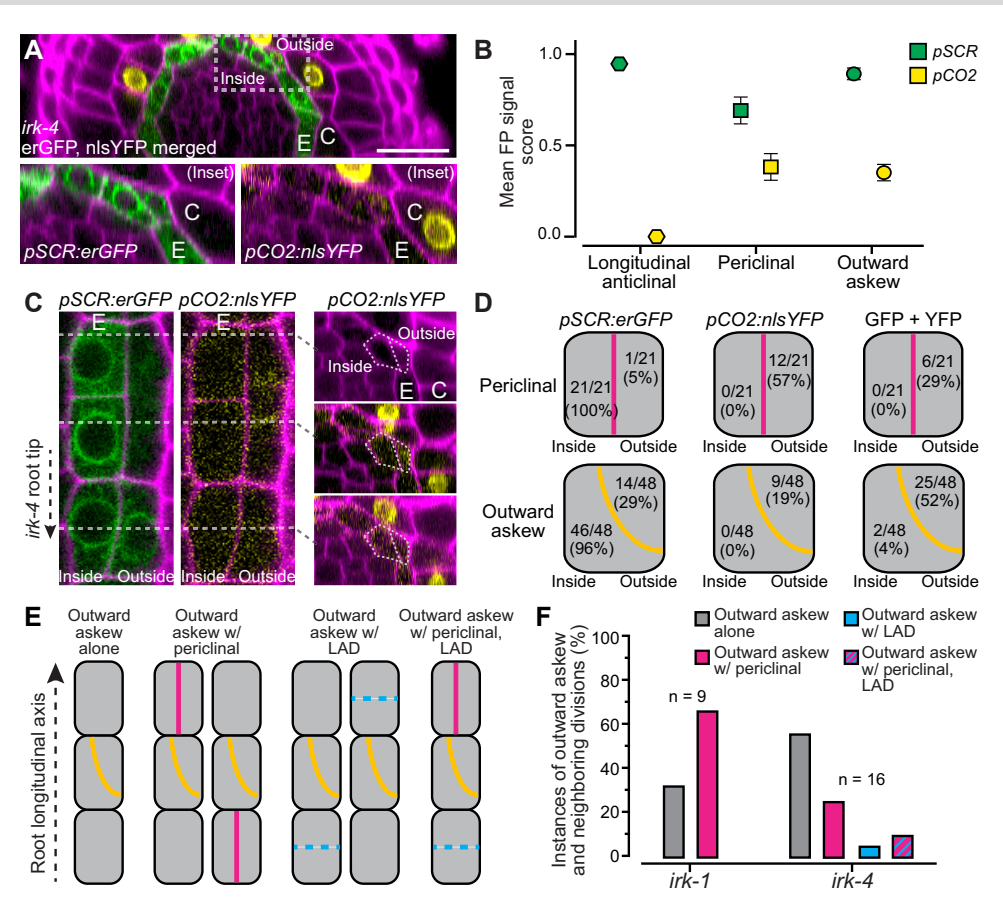


Figure 5. The peripheral daughters of outward askew endodermal divisions in irk-4 acquire cortex cell identity. **A)** Confocal micrograph showing portion of a transverse section of an irk-4 root meristem stained with propidium iodide (PI, magenta) and simultaneously expressing the pSCARECROW: endoplasmic reticulum-localized-green fluorescent protein (pSCR:erGFP) and pCORTEX2:nuclear localized yellow fluorescent protein (pCO2:nlsYFP), reporters for endodermis (E, green) and cortex (C, yellow), respectively. Dashed rectangle indicates inset region (lower panels) showing an outward askew endodermal division with each reporter shown separately. Scale bar: $25 \,\mu$ m. **B)** Mean fluorescent signal score (based on subjective intensity) from cell identity reporters in the daughter cells of longitudinal anticlinal divisions (LADs, n=44), periclinal divisions (n=42), and outward askew divisions (n=92). Obvious signal = 1, weak signal = 0.5, no signal = 0. Error bars show standard error of the mean. **C)** Longitudinal (left, center) and transverse (right) sections showing progressive accumulation of pCO2:nlsYFP in the outer daughter cell of an outward askew division in the longitudinal axis of an irk-4 root. **D)** Frequency of exclusive expression of cell identity markers (left, center) and incidence of their co-expression (right) in the daughter cells of periclinal and outward askew divisions (n=9 roots). **E)** Diagrams of endodermal cell files with an outward askew division (center cell, orange line) neighbored by cells that have not divided (left) or have undergone a periclinal (magenta line, left center) or longitudinal anticlinal division (LAD, cyan dashed line as these divisions are not visible in the longitudinal axis, right center) or both (right). **F)** Bar graph showing instances of outward askew endodermal divisions in irk with the neighboring cell states (as shown in E) as a proportion of the total instances per genotype (8 roots per genotype, irk-1: 9 instances; irk-4: 16 instances). See the methods secti

linked and tightly controlled. The role of IRK in this process is particularly compelling when the spatial relationship between the irk cell division orientation defects and IRK polar accumulation is considered (Fig. 6, A and B). In the endodermis of irk-1 or irk-4 IRKAK-GFP roots, a portion of IRK is present at the outer lateral domain of the PM, and there are fewer outward askew and LADs, but more periclinal divisions than in irk-4. In those genotypes, excess endodermal cell divisions are present but the division planes contact the outer lateral endodermal face infrequently. Whereas in irk-4, the putative null allele, excess endodermal divisions are very frequently oriented such that the division plane contacts the outer lateral face (Fig. 6C). Therefore, the presence of IRK and, to some extent, IRKAK at the outer lateral endodermal face has a negative influence on the selection of particular division planes.

To instruct cell division plane orientation, a polar-localized protein would need to influence the positioning of the cell division machinery. In plants, this includes the mitotic spindle and 2 plant-specific cytoskeletal structures, the preprophase band, which

marks the future division site, and the phragmoplast, which assembles and guides cell plate formation (Rasmussen et al. 2013; Smertenko et al. 2017). Many studies have investigated the mechanisms underlying how a new cell plate is attracted to the marked division site. However, our findings are consistent with a mechanism that repels cell plates from particular sites. We predict dueling attractive and repulsive cues would increase the precision and robustness of the cell division orientation process. For instance, in the ton recruiting motif (trm) 6,7,8 triple mutant the preprophase band is not detectable, yet the defects in root cell division orientation and stomata patterning are modest (Schaefer et al. 2017). This hints that other mechanisms exist to position division planes and there is increasing evidence that polarized proteins can directly and/or indirectly position division planes via linkage with the cytoskeleton. For example, during stomatal development, BASL/ BRX family polarity domain depletes cortical microtubules at particular positions ensuring the preprophase band forms outside the site marked by this polarity domain (Muroyama et al. 2020; Muroyama et al. 2023). Identification of the molecular links

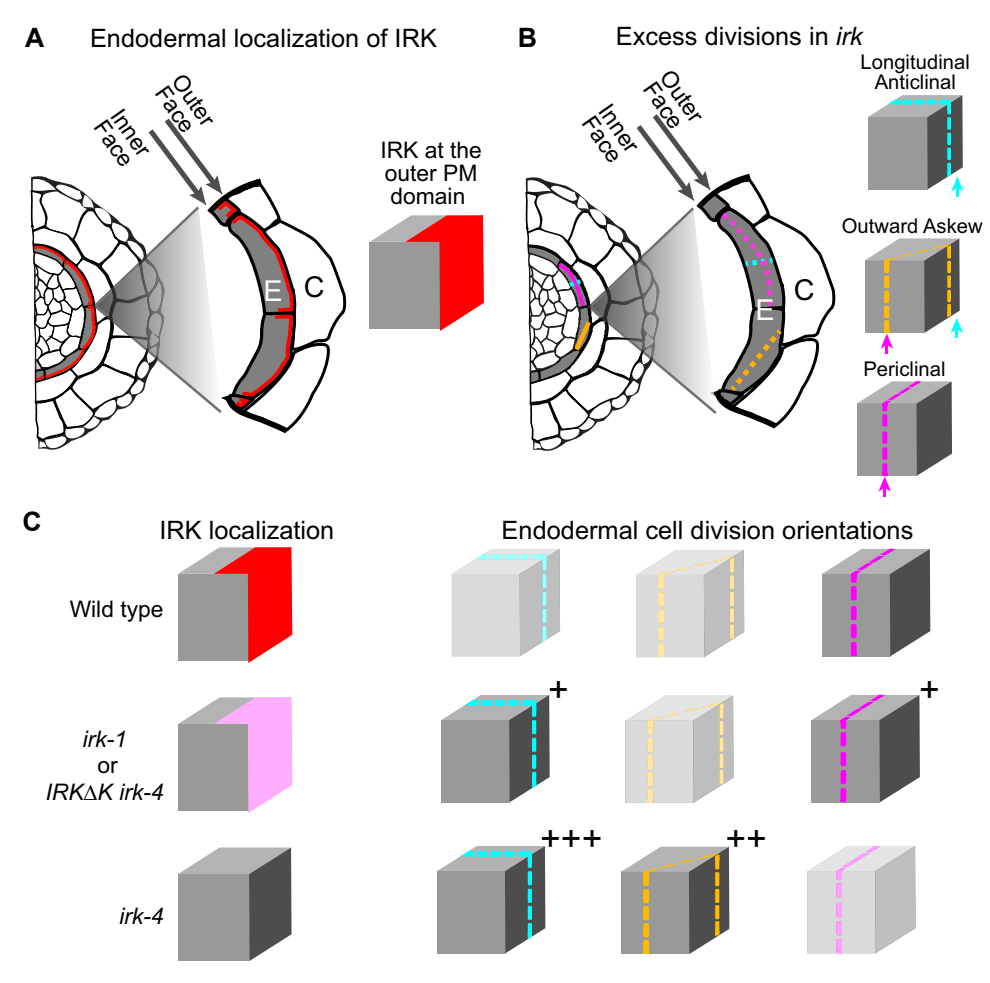


Figure 6. Linking IRK polar localization to endodermal division orientations in irk. Schematics of A) INFLORESCENCE AND ROOT APICES RECEPTOR KINASE (IRK) localization (red) at the outer lateral endodermal (E) cell face and B) excess endodermal division orientations in irk. Cortex (C) cell layer labeled for reference. C) Schematics of single endodermal cells, represented as cubes, showing IRK localization (left) and endodermal division phenotypes (right) in the various genotypes. Plus (+) signs indicate the extent to which divisions in each of these orientations are present in irk compared to Wild type. The faded division orientations are rarely observed or, in the mutants, are not present at greater numbers than in Wild type. Excess endodermal cell divisions in irk-4 are frequently oriented such that the division plane contacts the endodermal cell face where IRK resides in Wild type, irk-1, and irk-4 expressing the IRKAK reporter.

between IRK and the mechanics of cell division orientation and/or cytokinesis are key avenues of future investigation.

Outward askew endodermal divisions often spatially correlate with periclinal divisions and their peripheral daughters progressively acquire cortex identity, suggesting that they are formative in nature. Formative plant cell divisions often must traverse a longer path than proliferative divisions, which typically occur along the shortest path that divides the cell equally (Besson and Dumais 2011; Facette et al. 2018; Rasmussen and Bellinger 2018); indeed, the path of an endodermal periclinal division is the longest in this cell type. Therefore, a simple conclusion is that outward askew endodermal divisions are just misoriented periclinal divisions. This would suggest IRK is needed to maintain division orientation parallel to the outer lateral face during "long path" endodermal formative divisions. However, contemplating IRK function only in the context of maintaining the orientation of formative, periclinal endodermal divisions due to the long division path fails to account for the excess endodermal LADs, which can also be considered "long path" divisions and are a key attribute of the irk

Moreover, outward askew divisions are often flanked by endodermal cells that have not divided at all. Comparing the instances of outward askew endodermal divisions in irk-4 flanked by no division, an LAD, or a periclinal division to the average number of outward askew divisions per root, reveals that outward askew divisions occur in consecutive stretches along endodermal cell files. If they were simply misoriented periclinal divisions, we might expect them to be more interspersed with properly oriented periclinal divisions. If they are not simply misoriented periclinal divisions—could outward askew divisions be a distinctly oriented formative endodermal cell division? Two details hint at this, first, in addition to always being at the periphery of the endodermis, the daughters of outward askew endodermal divisions very often occur at the position where 2 cortex cells circumferentially meet (e.g. Figure 1, C and 5A). Second, besides the endodermal cell division defects, the stele area of irk roots, particularly irk-4, is substantially wider than Wt due to increases in cell size (Campos et al. 2020; Goff et al. 2023). This likely increases the mechanical force on the peripheral cell layers and cell division orientations are altered in response to changes in mechanical tension (Shapiro et al. 2015; Louveaux et al. 2016; Marhava et al. 2019). Thus, outward askew endodermal divisions could be a distinct and specific division orientation that generates precisely placed cells poised to invade the cortex layer to accommodate root widening.

We show extensive activity of pCYCD6; 1 in irk roots and, consistent with its reported activity in Wt, it is associated with formative GT divisions (Sozzani et al. 2010). However, pCYCD6; 1 activity also strongly associates with endodermal LADs, which are proliferative divisions. It is possible that excess pCYCD6; 1 activity in irk mutants simply reflects the high number of endodermal cell divisions occurring at any one time and a general defect in spatiotemporal control of cell cycle activity. Persistent expression of cell cycle genes after cytokinesis could explain the excess endodermal cell divisions observed in irk mutants. However, there is no increase in (proliferative) transverse anticlinal endodermal divisions that would lengthen the irk root meristem (Campos et al. 2020), nor are these divisions associated with pCYCD6; 1 activity. Because all of the excess divisions in irk are oriented such that they broaden the root's radial axis and are associated with pCYCD6; 1 activity, we propose that IRK represses a GT cell division program specific to the root's radial axis with CYCD6; 1 downstream of IRK in this pathway.

In developmental biology, cell divisions are categorized into 2 groups: formative and proliferative. Formative divisions are considered to be special, requiring cues to initiate and properly orient; in plants, this often occurs in the long axis of the cell and creates an additional cell layer with a distinct identity. In contrast, proliferative plant cell divisions tend to occur along the shortest path to create equally sized daughter cells of the same identity. It is straightforward to suggest that distinct mechanisms regulate proliferative and formative divisions. However, this is not very satisfying when considering the endodermal divisions linked to IRK and CYCD6; 1. While neither IRK nor CYCD6; 1 have known roles in proliferative cell divisions in the root's longitudinal axis (Sozzani et al. 2010; Campos et al. 2020), they are linked to proliferative divisions in the radial axis. This implies that, in addition to the differential regulation between proliferative and formative divisions, distinctly oriented proliferative divisions are also differentially regulated from each other. However, a more parsimonious explanation may be that root cells separately regulate divisions that occur in different orientations. While this may seem more complex than the currently accepted formative vs. proliferative division paradigm, it may be more aligned with the underlying logic of plant body plan elaboration with respect to its organ axes. Consistent with this, our study of IRK indicates that a distinct pathway operates to repress cell divisions that specifically broaden the radial axis of the root GT—whether those divisions are proliferative or formative.

Materials and methods Plant material and growth conditions

Seeds were surface sterilized with chlorine gas and plated on MS agar media. The media contained 0.2 x Murashige and Skoog salts (Caisson labs), 0.5 g/L MES, 1% w/v Sucrose, and 1% agar (Difco) and was at pH 5.7. Plates were sealed with parafilm and placed at 4°C for 24 to 72 h for stratification. After stratification, plates were placed vertically in a Percival incubator and grown under 16 h light/8 h dark at a constant temperature of 22°C. For each experiment, the genotypes being analyzed were grown side-by-side on the same plate with 2 to 3 plates grown and analyzed together for each replicate. Thus, each plate is considered a technical replicate and separate repeats of the experiments as biological replicates. Arabidopsis (Arabidopsis thaliana) ecotype Col-0 was used as the Wild type (Wt). The genotypes irk-1, irk-4, irk-4 pIRK:IRK:IKK:GFP, and irk-4 pIRK:IRK:GFP were obtained as previously described

(Campos et al. 2020; Rodriguez-Furlan et al. 2022). The cell type-specific reporters pCO2:nlsYFP (Paquette and Benfey 2005), pSCR: erGFP (Di Laurenzio et al. 1996; Wysocka-Diller et al. 2000), and pCYCD6; 1::GUS:GFP [endoplasmic reticulum-localized GFP, erGFP (Sozzani et al. 2010)] were received from the Benfey lab and were crossed the irk mutants as previously described (Campos et al. 2020).

Confocal microscopy and image analysis

Roots were imaged at day 6 post-stratification (dps) and stained with ~10 μ M propidium iodide (PI) solubilized in water for 1 to 2 min; then, they are imaged on a Leica SP8 upright microscope and imaging system housed in the Van Norman lab. Fluorescent protein (FP) signals were captured using the following settings: PI (excitation, 536 nm; emission, 585 to 660 nm) and GFP/YFP (excitation, 488 nm; emission, 492 to 530 nm). Z-stacks were acquired and analyzed with the orthogonal sectioning tool of the LASX software. The total number of endodermal divisions per root was counted from the QC to QC +120 μ m or 20 cells as previously described (Campos and Van Norman 2022). Representative images of roots expressing the pCYCD6; 1:GUS:GFP, pSCR:erGFP, and pCO2:nls:YFP reporters were acquired from a transverse optical section at the 10th endodermal cell (E10) shootward of the QC.

Signal separation GFP/YFP was performed by linear unmixing of a spectral image (Zimmermann et al. 2014), acquired with an inverted Zeiss 880 microscope with 32 channel spectral detector, objective 40X/1.2 W Korr FCS M27, MBS 488/561 and exciting with both 561 and 488 nm. Signal was collected simultaneously in 18 channels from 463 to 624 nm in ~9 nm bands. GFP/YFP and PI signal was subsequently separated using Zeiss ZEN software linear unmixing tools.

For the images used to quantify endodermal cell divisions and generate the endodermal cell division map (see below), Z-stacks were acquired from each root at 512×512 pixels with $1\,\mu\mathrm{m}$ between optical sections. All 3 genotypes expressing a single reporter were grown on the same plate, 14–15 plants per genotype were imaged, and ≥ 10 plants per genotype were analyzed in detail. For each root, the optical sections were manually analyzed from the QC shootward 20 endodermal cells (E1 to 20), such that >160 endodermal cells per root were examined for excess endodermal cell divisions.

Generation of the paired point graphs and endodermal cell division maps

To generate the endodermal cell division maps for each genotype, we examined promoter activity and the presence of periclinal, outward askew, and longitudinal anticlinal divisions in each optical transverse section from just above the QC shootward to endodermal cell position 20 (E20). If a division was present, we documented whether the daughter cell was positive or negative for the reporter. For plants expressing pCYCD6; 1:erGFP, we examined endodermal LADs, periclinal, and outward askew divisions. For plants expressing pSCR:erGFP and pCO2:nls:YFP, we only examined the endodermal periclinal and outward askew divisions, as the daughters of endodermal LADs remain endodermal cells. The total number of these divisions was quantified per root and then counted as FP positive (+) or negative (-). A summary of these data for each reporter is displayed in paired point graphs, where the number of FP + and FP- cells from a single root are connected by a dotted line. This shows the precise number of divisions per root in each genotype but lacks the spatial information present in the cell division maps (see description below). We note that the excess periclinal endodermal division phenotype in irk-1 appears slightly repressed in the reporter backgrounds (compare Fig. 1F to Supplementary Figs. S1B and S2B, and S3B); however, this is likely due to general variability in the number of periclinal divisions in any genotype and relatively low number of roots $(n = \sim 40 \text{ vs.} \sim 10, \text{ respectively})$ examined per replicate.

The endodermal cell division map shows whether periclinal, outward askew, and/or longitudinal anticlinal divisions were present at a given position (E1 to E20). This information is compressed, as the map does not include the absolute number of divisions or map divisions in the root's radial axis. Specifically, if a box in the division map is a solid color, then all the daughter cells for a given endodermal division that is present expressed the reporter —whether there was a single division or several. If some, but not all, of the daughter cells expressed the reporter, then the box in the map has a gradient fill. Finally, if none of the daughter cells expressed the reporter the box is unfilled (white). Endodermal division orientations are represented by different shapes in each box in the endodermal cell division maps: LADs are indicated by a black arrowhead on the right, internal side; periclinal divisions are indicated by a black arrowhead on the lower, internal side, and outward askew divisions are indicated by a curved line in the lower-right corner. If none of these endodermal cell divisions were detected, the box is empty.

Assessing the spatial correlation between endodermal division orientations

To determine if endodermal outward askew divisions were correlated with periclinal or longitudinal anticlinal division, the endodermal cell division pattern along the root's longitudinal axis was examined in each genotype expressing pCYCD6; 1:GUS:GFP. In endodermal cell files from the QC upwards, transverse optical sections were examined for an outward askew division; then the adjacent shootward and rootward cells were examined for an abnormal division or no division. If the adjacent cell also had an outward askew division, we proceeded to look until an endodermal cell that had a periclinal or longitudinal anticlinal division or no division was found up to E20 for all cell files.

Figure generation

Confocal images were exported from Leica software (LASX) as TIF files, which were cropped and resized in Adobe Photoshop. Graphs were generated with PRISM8 (GraphPad software https://www.graphpad.com/, San Diego, USA). Schematics were created in Adobe Illustrator. The figures containing confocal images, graphs, and schematics were assembled in Adobe Illustrator.

Acknowledgments

We thank former members of the Van Norman lab, including J.G., J.N.T., and C.R.F., and C.R. [UC, Riverside (UCR)] for discussions of and feedback on this manuscript while it was in preparation. We also thank P.S. (UCR) for her insightful suggestion for how to display the endodermal division map. We appreciate access to the Zeiss 880 confocal microscope housed in the Institute of Integrative Genome Biology Microscopy Core Facility (UCR).

Author contributions

Conceptualization: R.C., J.M.V.N., and R.M.I.K.R.; cell division methodology: R.C.; endodermal division & FP mapping: R.M.I.K.R. and R.C.; dual FP examination: P.P.H.; resources: J.M.V.N. and R.C.;

writing/editing—original draft: J.M.V.N., R.C., R.M.I.K.R., and P.P.H.; revision: J.M.V.N.; visualization: J.M.V.N., R.M.I.K.R., R.C., and P.P.H.; supervision: J.M.V.N.; funding acquisition: J.M.V.N.

Accession numbers

Sequence data from this article can be found in the GenBank/EMBL data libraries under accession numbers At3g56370.

Supplementary data

The following materials are available in the online version of this article.

Supplementary Figure S1. Periclinal divisions are often associated with pCYCD6; 1 activity.

Supplementary Figure S2. Periclinal endodermal division daughter cells often show pSCR activity.

Supplementary Figure S3. Periclinal endodermal division daughter cells occasionally show pCO2 activity.

Funding

This work was supported by funds from University of California, Riverside, including Initial Complement (IC) and Academic Senate funds, USDA-NIFA-CA-R-BPS-5156-H, and NSF CAREER #1751385 awarded to JMVN. Publication costs were paid with funds from University of California, Los Angeles.

Conflict of interest statement. None declared.

Data availability

The data underlying this article will be shared on reasonable request to the corresponding author.

References

Besson S, Dumais J. Universal rule for the symmetric division of plant cells. Proc Natl Acad Sci U S A. 2011:108(15):6294–6299. https://doi.org/10.1073/pnas.1011866108

Campos R, Goff J, Rodriguez-Furlan C, Van Norman JM. The Arabidopsis receptor kinase IRK is polarized and represses specific cell divisions in roots. *Dev Cell*. 2020:52(2):183–195.e4. https:// doi.org/10.1016/j.devcel.2019.12.001

Campos R, Van Norman JM. Confocal analysis of Arabidopsis root cell divisions in 3D: a focus on the endodermis. *Methods Mol Biol.* 2022:2382:181–207. https://doi.org/10.1007/978-1-0716-1744-1_11

Cui H. Middle Cortex formation in the root: an emerging picture of integrated regulatory mechanisms. *Mol Plant.* 2016:9(6):771–773. https://doi.org/10.1016/j.molp.2016.05.002

De Smet I, Beeckman T. Asymmetric cell division in land plants and algae: the driving force for differentiation. Nat Rev Mol Cell Biol. 2011:12(3):177–188. https://doi.org/10.1038/nrm3064

Di Laurenzio L, Wysocka-Diller J, Malamy JE, Pysh L, Helariutta Y, Freshour G, Hahn MG, Feldmann KA, Benfey PN. The SCARECROW gene regulates an asymmetric cell division that is essential for generating the radial organization of the Arabidopsis root. *Cell.* 1996:86(3):423–433. https://doi.org/10.1016/S0092-8674(00)80115-4

Dolan L, Janmaat K, Willemsen V, Linstead P, Poethig S, Roberts K, Scheres B. Cellular organisation of the Arabidopsis thaliana root. Development. 1993:119(1):71–84. https://doi.org/10.1242/dev. 119.1.71

- Facette MR, Rasmussen CG, Van Norman JM. A plane choice: coordinating timing and orientation of cell division during plant development. *Curr Opin Plant Biol.* 2018:47:47–55. https://doi.org/10.1016/j.pbi.2018.09.001
- Goff J, Imtiaz Karim Rony R, Ge Z, Hajný J, Rodriguez-Furlan C, Friml J, Van Norman JM. PXC2, a polarized receptor kinase, functions to repress ground tissue cell divisions and restrict stele size. bioRxiv 429611, https://doi.org/10.1101/2021.02.11.429611, 19 March 2023, preprint: not peer reviewed.
- Hartman KS, Muroyama A. Polarizing to the challenge: new insights into polarity-mediated division orientation in plant development. *Curr Opin Plant Biol.* 2023:74:102383. https://doi.org/10.1016/j.pbi. 2023.102383
- Heidstra R, Welch D, Scheres B. Mosaic analyses using marked activation and deletion clones dissect Arabidopsis SCARECROW action in asymmetric cell division. *Genes Dev.* 2004:18(16): 1964–1969. https://doi.org/10.1101/gad.305504
- Livanos P, Müller S. Division plane establishment and cytokinesis. Annu Rev Plant Biol. 2019:70(1):239–267. https://doi.org/10.1146/annurev-arplant-050718-100444
- Louveaux M, Julien J-D, Mirabet V, Boudaoud A, Hamant O. Cell division plane orientation based on tensile stress in Arabidopsis thaliana. Proc Natl Acad Sci U S A. 2016:113(30):E4294–E4303. https://doi.org/10.1073/pnas.1600677113
- Marhava P, Hoermayer L, Yoshida S, Marhavý P, Benková E, Friml J. Re-activation of stem cell pathways for pattern restoration in plant wound healing. *Cell.* 2019:177(4):957–969.e13. https://doi.org/10.1016/j.cell.2019.04.015
- Muroyama A, Gong Y, Bergmann DC. Opposing, polarity-driven nuclear migrations underpin asymmetric divisions to pattern Arabidopsis stomata. *Curr Biol.* 2020:30(22):4467–4475.e4. https://doi.org/10.1016/j.cub.2020.08.100
- Muroyama A, Gong Y, Hartman KS, Bergmann DC. Cortical polarity ensures its own asymmetric inheritance in the stomatal lineage to pattern the leaf surface. Science. 2023:381(6653):54–59. https://doi.org/10.1126/science.add6162
- Paquette AJ, Benfey PN. Maturation of the ground tissue of the root is regulated by gibberellin and SCARECROW and requires SHORT-ROOT. Plant Physiol. 2005:138(2):636–640. https://doi.org/10.1104/pp.104.058362
- Pillitteri LJ, Guo X, Dong J. Asymmetric cell division in plants: mechanisms of symmetry breaking and cell fate determination. *Cell Mol Life* Sci. 2016:73(22):4213–4229. https://doi.org/10.1007/s00018-016-2290-2
- Rasmussen CG, Bellinger M. An overview of plant division-plane orientation. *New Phytol.* 2018:219(2):505–512. https://doi.org/10.1111/nph.15183
- Rasmussen CG, Humphries JA, Smith LG. Determination of symmetric and asymmetric division planes in plant cells. *Annu Rev Plant Biol.* 2011:62(1):387–409. https://doi.org/10.1146/annurevarplant-042110-103802
- Rasmussen CG, Wright AJ, Müller S. The role of the cytoskeleton and associated proteins in determination of the plant cell

- division plane. Plant J. 2013:75(2):258–269. https://doi.org/10.1111/tpi.12177
- Rodriguez-Furlan C, Campos R, Toth JN, Van Norman JM. Distinct mechanisms orchestrate the contra-polarity of IRK and KOIN, two LRR-receptor-kinases controlling root cell division. *Nat Commun.* 2022:13(1):235. https://doi.org/10.1038/s41467-021-27913-1
- Schaefer E, Belcram K, Uyttewaal M, Duroc Y, Goussot M, Legland D, Laruelle E, de Tauzia-Moreau M-L, Pastuglia M, Bouchez D. The preprophase band of microtubules controls the robustness of division orientation in plants. Science. 2017:356(6334):186–189. https://doi.org/10.1126/science.aal3016
- Scheres B, Benfey PN. ASYMMETRIC CELL DIVISION IN PLANTS.

 Annu Rev Plant Physiol Plant Mol Biol. 1999;50(1):505–537. https://doi.org/10.1146/annurev.arplant.50.1.505
- Shapiro BE, Tobin C, Mjolsness E, Meyerowitz EM. Analysis of cell division patterns in the Arabidopsis shoot apical meristem. Proc Natl Acad Sci U S A. 2015:112(15):4815–4820. https://doi.org/10.1073/pnas.1502588112
- Shiu SH, Bleecker AB. Receptor-like kinases from Arabidopsis form a monophyletic gene family related to animal receptor kinases. Proc Natl Acad Sci U S A. 2001:98(19):10763–10768. https://doi.org/10.1073/pnas.181141598
- Shiu SH, Bleecker AB. Expansion of the receptor-like kinase/pelle gene family and receptor-like proteins in Arabidopsis. Plant Physiol. 2003:132(2):530–543. https://doi.org/10.1104/pp.103.021964
- Smertenko A, Assaad F, Baluška F, Bezanilla M, Buschmann H, Drakakaki G, Hauser M-T, Janson M, Mineyuki Y, Moore I, et al. Plant cytokinesis: terminology for structures and processes. Trends Cell Biol. 2017:27(12):885–894. https://doi.org/10.1016/j.tcb.2017.08.008
- Sozzani R, Cui H, Moreno-Risueno MA, Busch W, Van Norman JM, Vernoux T, Brady SM, Dewitte W, Murray JAH, Benfey PN. Spatiotemporal regulation of cell-cycle genes by SHORTROOT links patterning and growth. *Nature*. 2010:466(7302):128–132. https://doi.org/10.1038/nature09143
- van den Berg C, Willemsen V, Hage W, Weisbeek P, Scheres B. Cell fate in the Arabidopsis root meristem determined by directional signalling. *Nature*. 1995:378(6552):62–65. https://doi.org/10.1038/378062a0
- Van Norman JM. Asymmetry and cell polarity in root development. *Dev* Biol. 2016:419(1):165–174. https://doi.org/10.1016/j.ydbio.2016.07.009
- Wallner E-S. The value of asymmetry: how polarity proteins determine plant growth and morphology. *J Exp Bot.* 2020:71(19): 5733–5739. https://doi.org/10.1093/jxb/eraa329
- Wysocka-Diller JW, Helariutta Y, Fukaki H, Malamy JE, Benfey PN. Molecular analysis of SCARECROW function reveals a radial patterning mechanism common to root and shoot. *Development*. 2000:127(3):595–603. https://doi.org/10.1242/dev.127.3.595
- Zimmermann T, Marrison J, Hogg K, O'Toole P. Clearing up the signal: spectral imaging and linear unmixing in fluorescence microscopy. In: Paddock SW, editors. Confocal microscopy: methods and protocols. New York, NY: Springer; 2014. p. 129–148.